RESEARCH ARTICLE | OCTOBER 06 2023

Adoption of CO_2 mixtures as working fluid for CSP cycles with linear collectors and molten salts as HTF

Ettore Morosini; Marco Binotti; Gioele Di Marcoberardino; Costante Invernizzi; Paolo Iora; Giampaolo Manzolini

AIP Conf. Proc. 2815, 110002 (2023)
https://doi.org/10.1063/5.0149565

Adoption of CO_2 Mixtures as Working Fluid for CSP Cycles With Linear Collectors and Molten Salts as HTF

Ettore Morosini[1, a)], Marco Binotti[1], Gioele Di Marcoberardino[2], Costante Invernizzi[2], Paolo Iora[2], Giampaolo Manzolini[1]

[1]*Politecnico di Milano, Department of Energy, via Lambruschini 4A, 20156, Milan, Italy*
[2]*Università degli Studi di Brescia, via Branze 38, Brescia, Italy*

[a)] Corresponding author: ettore.morosini@polimi.it

Abstract. This work deals with the adoption of CO_2-based mixtures as working fluid in transcritical cycles for CSP applications. A direct comparison with the small-scale CSP plant based on a Rankine cycle operating in Partanna (Italy) is developed to verify the potential advantages of the proposed novel cycles both in design conditions and on yearly basis. The solar plant consists of linear Fresnel reflectors using solar salts as HTF and a large direct thermal energy storage. The solar to thermal performances of the power plant are evaluated with the software SAM, while the design of the cycle with the innovative working fluids (CO_2+C_6F_6 and CO_2+$C_6F_{12}O$) is developed in ASPEN Plus. An annual analysis based on hourly DNI data is then performed to assess the yearly electricity yield together with a preliminary economic analysis. The results of the most advanced cycle layout exploiting the innovative working fluid evidence a minor reduction of the computed LCOE when compared to the traditional technology (around 10%), a result highly sensitive to the power block costs, and a 2GWh increment in the yearly energy produced (13% of the Rankine production).

INTRODUCTION

The current research on CSP plants is mainly focused on large scale solar tower plants using innovative high temperature receivers and advanced sCO_2 cycles as power conversion technology [1]. A further potential improvement of the cycle conversion efficiency is expected with the adoption of CO_2-based mixtures as working fluid: this solution is currently investigated for large scale high temperature solar tower applications within the H2020 project SCARABEUS [2]. As a matter of fact, an important limitation of sCO_2 cycles used for CSP applications is their drop in cycle efficiency at high ambient temperatures, a typical situation when an air-cooled condenser is adopted.

A solution to this problem can be turning supercritical cycles into transcritical ones, adopting a pump instead of a compressor for the compression step: this requires blending pure CO_2 with a dopant so that the critical temperature of the mixture can rise at least up to 70°C. The required dopant would need to have a critical temperature well above the one of CO_2, so that a small amount of it in the mixture is sufficient to bring the compression region in liquid phase.

The innovative working fluids proposed in this work are the CO_2+C_6F_6 mixture and the CO_2+ $C_6F_{12}O$ mixture: the dopants are chosen according to their critical temperature (243°C for C_6F_6 and 169°C for $C_6F_{12}O$), to enable condensation for high cycle minimum temperatures. The selected dopants, moreover, should be thermally stable up to the maximum cycle temperatures, should not be toxic nor reactive and should ideally present a relatively low cost. In addition to these basic characteristics, a reliable thermodynamic assessment of the mixture as working fluid would require at least some additional experimental data of the mixture such as its vapor liquid equilibrium (VLE) behavior.

C_6F_6 and $C_6F_{12}O$ are hence selected as suitable dopants for CO_2 mixtures since they comply with the mentioned criteria: $C_6F_{12}O$ is a fluid already on the market, used both as HTF and working fluid, and its health and flammabilty hazards are completely negligible. For these reasons, it can be considered of interest and competitive with respect to C_6F_6, a more unconventional working fluid, with a low toxicity and a relatively low flammabilty. Previous works on CO_2 mixtures as working fluids tried to explore other mixtures such as the CO_2+$TiCl_4$ or the CO_2+N_2O_4 mixture [3]. The advantage of the dopants selected in this works, then, is the reduced health hazard of the dopant themselves.

SolarPACES: Solar Power & Chemical Energy Systems
AIP Conf. Proc. 2815, 110002-1–110002-9; https://doi.org/10.1063/5.0149565
Published by AIP Publishing. 978-0-7354-4623-6/$30.00

The scope of this work is to analyze these CO_2-based mixtures as working fluid for small-scale power cycles coupled with linear Fresnel reflectors: for similar applications and sizes, indeed, valid cycles alternatives are commercially deployed, such as ORC or steam cycles [4]. Here, the adoption of steam Rankine cycles and transcritical cycles with CO_2 mixtures is investigated, focusing on both the investigation of the optimal plant layout configuration and the gain in cycle efficiency of the innovative solutions with respect to traditional ones. Finally, an off design of the power block at various ambient temperatures is proposed, as it is necessary to compute the yearly energy produced.

SOLAR FIELD DESCRIPTION AND PLANT PERFORMANCES

The solar field adopted in this work aims at mimicking the characteristics of the power plant installed in Partanna (Italy) starting from early 2019 under the supervision of the Italian research center ENEA [5] in a location characterized by a relatively low yearly DNI, in the order of 1800 kWh/m^2/y. The solar plant adopts linear Fresnel reflectors and it exploits a direct storage system with molten salts. The solar plant is schematized in Figure 1, while the thermal and optical properties of the collectors and receivers are listed in Table 1. The maximum working fluid temperature is 530°C for steam and the C_6F_6 mixture, while it is limited to 475°C for the $C_6F_{12}O$ mixture due to thermal stability limits: a study on this mixture, in fact, evidenced only a very limited degradation of the fluid at 475°C after 10 hours, while the complete decomposition occurs at 550°C [6].

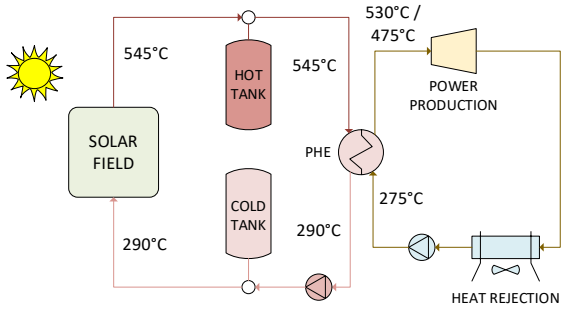

FIGURE 1. Solar plant layout analyzed.

TABLE 1. Review of the main characteristics of the solar field and the assumptions of its thermal and optical performances.

Characteristics	Description	Parameter	Value
Location	Partanna, Italy	Absorber absorptance	96%
PHE Thermal power	12 MW	Envelope absorptance	2%
TES	15 h – Solar salts	Glass envelope emissivity	86%
HTF Temperatures	290°C / 545 °C	Envelope transmittance	96.3%
Working fluid temperature across the PHE	275°C / 530°C (Steam, CO_2+C_6F_6); 475°C (CO_2+ $C_6F_{12}O$)	Optical efficiency at design	65.0%
		Thermal loss at design	150 W/m
Solar field / Collector area	83000 m^2 / 660 m^2	Thermal efficiency at design	98.3%
Collector type	FRENELL	Piping thermal losses	0.45 W/m^{2}K

The reported characteristics are assumed using as reference the System Advisor Model (SAM v.2020 11.29) [7]. Following the same approach, the auxiliary consumptions (HTF pumps, collector drives, etc) and the TES and solar field thermal losses are taken from SAM, while the parasitic load for freeze protection is assumed accordingly to ENEA [5]. For this system, considering SAM weather data of 2017, 2018 and 2019 of that location, the resulting monthly solar resource and power transferred to the HTF are reported in Figure 2.

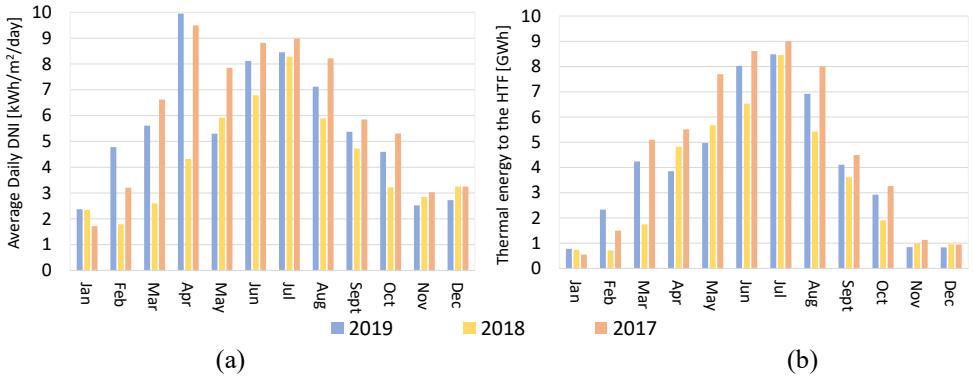

FIGURE 2. Partanna solar resources (a) and solar plant performances (b) in the period 2017-2019.

METHODOLOGY

The power cycle calculations of the two investigated mixtures are performed in ASPEN PLUS v.11: for the CO_2+C_6F_6 mixture the PC-SAFT equation of state (EoS) is adopted, optimized with binary interaction parameters on VLE data as reported in literature [8], while the CO_2+ $C_6F_{12}O$ mixture is modelled with the Peng Robinson EoS with Soave alpha function and k_{ij} equal to 0.073, optimized on VLE data [9]. The mixtures composition is determined maximizing the cycle efficiency: for this reason, a sensitivity analysis on the composition is performed in each case.

The assessment of the innovative working fluids aims at analyzing various efficient plant layouts that can fit the target temperature difference across the PHE (reported in Figure 1). The considered plant layouts are instead reported in Figure 3, selected among many for their high efficiency at low heat introduction temperature [10].

Among the three years of weather data considered, the results are presented for the year 2019, since it is the one denoting average values of DNI and thermal power transferred to the HTF between 2017, 2018 and 2019. Moreover, the thermal energy collected is coherent with what reported by ENEA (49.8GWh, according to ENEA, and 48.3 GWh for 2019 following this work assumptions). Considering the TES capacity, the yearly defocusing equivalent hours result around 127 h.

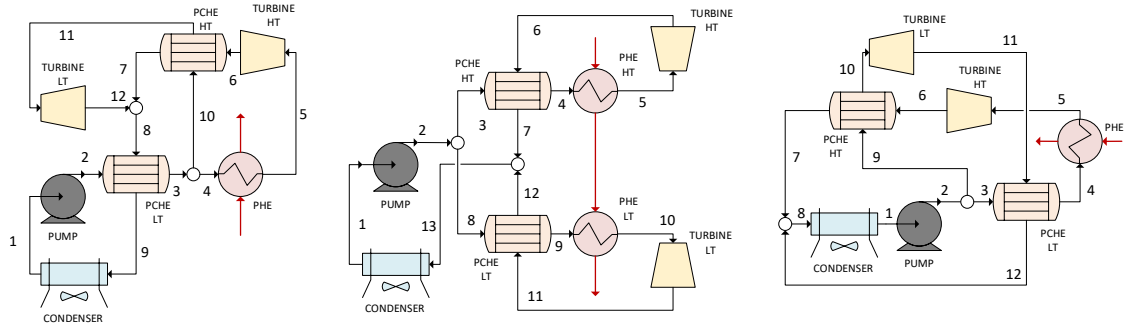

FIGURE 3. Selected plant layouts for transcritical cycle: Cascade cycle (a), Double simple cycle (b), Dual recuperative cycle (c).

Considering the annual performance of the cycles, while a tailored model for the Rankine cycle is employed using the software Thermoflex, the off-design performances of the CO_2-mixtures cycles are simulated at fixed cycle minimum temperature, considering simplified heat transfer correlations for finned air-cooled condensers. Moreover, the off-design analysis of the cycles is performed maximizing the energy production, always in full load configuration.

An economic analysis of the power block is also carried out, mostly using correlations from Weiland [11]: regarding the PHE, instead, the correlation from Carlson [12] is adopted, as no cost functions are reported in Weiland scaling the cost with UA_{PHE}. The pump cost is assumed as an average between the Weiland (for compressors) and the Carlson (for pump) correlation, due to a lack of reliable cost functions for pumps in compressible regions.

Wider uncertainties are instead foreseen in the prediction of the power block cost for the Rankine cycle: starting from SAM reference value of 1400\$/kW_{el} (representative of large-scale plants), a second value is also considered,

3000 \$/kW$_{el}$, in case a more costly and size-dependent cost correlation is preferred. Any intermediate value can be selected with a linear interpolation between these two extreme values, if considered of interest for the overall analysis. Furthermore, the different cycle configurations are compared according to their LCOE, defined in Eq. (1), where: the solar field cost are taken from SAM, the TES cost is fixed at 24 \$/kWh [13] and 22% of indirect and contingency costs are added, following SAM approach. The fixed OPEX are fixed at 72 \$/kW/y (also including the natural gas necessary for the freeze protection system), the variable OPEX at 4 \$/MWh and the CRF at 9.37%, (corresponding to an 8% discount rate). Figure 4 reviews the necessary step for the technoeconomic assessment carried out within this work.

$$LCOE\ \left[\frac{\$}{MWh}\right] = \frac{Total\ Plant\ CAPEX \cdot CRF + Fixed\ OPEX}{Yearly\ net\ Energy\ produced} + variable\ OPEX \tag{1}$$

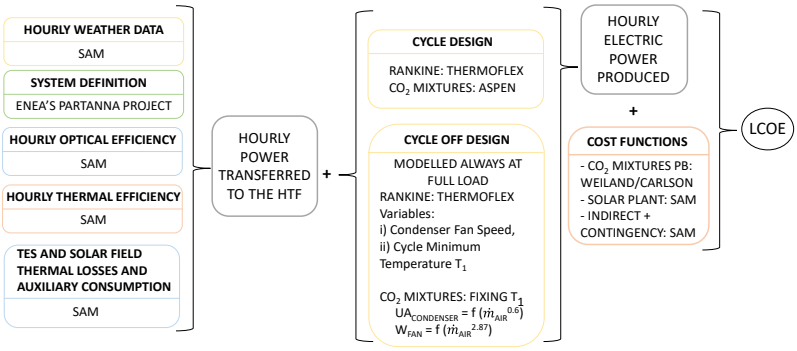

FIGURE 4. Overview of the methodology used to analyze the cycle performances of the different configurations.

POWER BLOCK MODELING AND PERFORMANCES

Steam Rankine Cycle

The model of a steam Rankine cycle with no reheat and four regenerative bleedings, similar to the one adopted in the Partanna plant [5], is designed using Thermoflex [14]. A schematic of the plant is reported in Figure 5, while the main design assumptions, taken from [5][15], are reported in Table 2. The turbine isentropic efficiency is varied in order to match the cycle gross power, while for the air-cooled condenser a ΔT of 15°C between air inlet temperature and condensing temperature is considered. The cycle off-design performance at variable ambient temperature is optimized by varying the air-cooled condenser fan rotational speed to maximize the cycle net power output as reported in Figure 7 (a) and optimizing the cycle minimum temperature, accordingly.

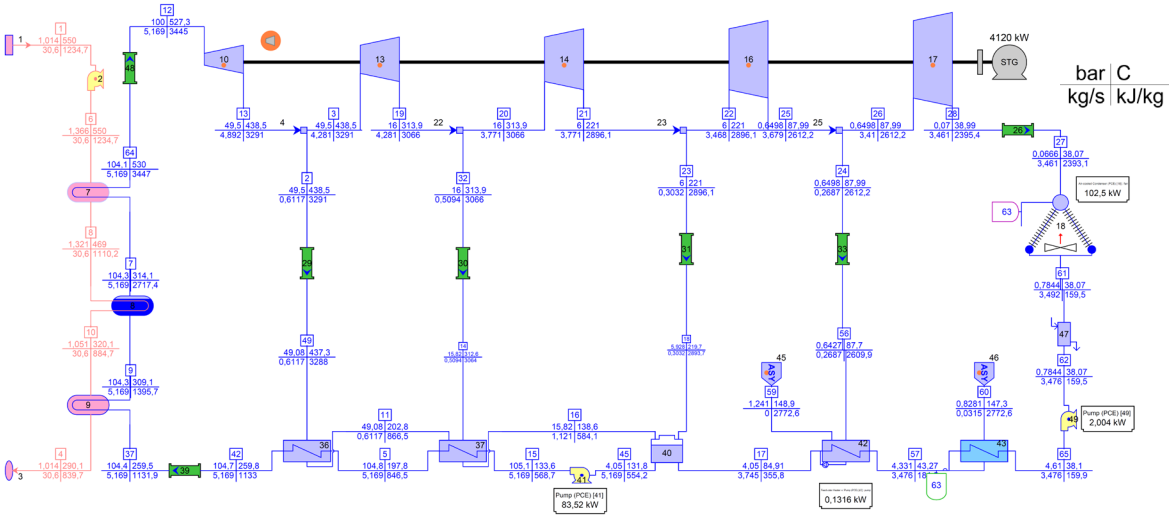

FIGURE 5. Plant layout of the steam Rankine cycle modelled in Thermoflex, similar to the one adopted in Partanna [5].

TABLE 2. Main design assumptions for the design of the steam Rankine cycle [5][15].

Parameter	Value	Parameter	Value
Maximum temperature/pressure	530°C /100 bar	Gross cycle efficiency	35.36%
Hot source temperatures	545°C/290°C	Turbine rotational speed	9400 rpm
Condensing pressure	0.067 bar	$\Delta T_{ColdEnd}$ Air cooled condenser	15°C
Cycle gross power	4.26 MW	Generator/Gearbox efficiency	98% / 98.6%

Transcritical CO_2 Mixtures Power Cycles

The innovative cycles are modelled in ASPEN PLUS assuming the cycle characteristics reported in

Table ***3*** (left) and referring to a cycle maximum pressure of 250 bar. The gross cycle efficiencies of the three working fluids are plotted in Figure 6 (a): for this application, the cascade cycle results the most efficient. For the two mixtures used in these configurations, the optimal molar fraction of CO_2 results around 80% for the $C_6F_{12}O$ mixture and in the range 86% to 90% for the mixture with C_6F_6: these best efficiency compositions are hence considered in this work and detailed in the following economic analysis.

The performances of the pure sCO_2 cycles (considering a maximum temperature of 530°C) are computed and reported on the bottom right of Figure 6 (a): the results are similar to the one of the Rankine cycle, as sCO_2 is not as performant as the mixtures for cycles with high and fixed temperature differences across the PHE.

Unlike the Rankine cycle, the off design of the transcritical cycles working with the mixtures is developed at fixed cycle minimum temperature, varying the air-cooled condenser fan speed. All the assumed characteristics of the air-cooled condenser are reported in

Table ***3*** (right) [16], including the auxiliary consumption of the condenser. Starting from the design conditions, for each different value of ambient temperature the condenser TQ diagram is discretized, and for each step the energy equation and the mean log temperature equation are solved together.

The off-design conditions of the condenser can hence be computed numerically, plotted in Figure 6 (b), where for each ambient temperature the outlet air temperature is defined: the figure depicts the off-design conditions where the ambient temperature is 10°C, 20°C and 38°C. In each of these conditions the outlet temperature of the air is different since the air mass flow rate varies, and a different air mass flow rate would entail different consumption of the air-cooled condenser.

TABLE 3. Assumptions on transcritical cycles characteristics (left), assumptions on the air-cooled condenser (right).

Parameter	Value	Parameter	Value
Minimum temperature	41°C	Design ambient temperature	31°C
Turbine isentropic efficiency	90%	Design ΔT_{AIR}	20°C
Pump isentropic efficiency	80%	$U_{OFF\ DESIGN}$ / U_{DESIGN}	$(\dot{m}_{AIR}/\dot{m}_{AIR\ DESIGN})^{0.6}$
ΔT_{MIN} of PCHEs	5°C	$W_{FAN-OFF\ DESIGN}/W_{FAN-DESIGN}$	$(\dot{m}_{AIR}/\dot{m}_{AIR\ DESIGN})^{2.78}$
ΔP_{PHE}	4 bar	Auxiliary consumption at design	$0.85\% \cdot Q_{cond}$
ΔP_{COND}	2 bar	Condenser model	Counter-current
$\Delta P_{PCHE-LP/HP}$	1/0.5 bar		

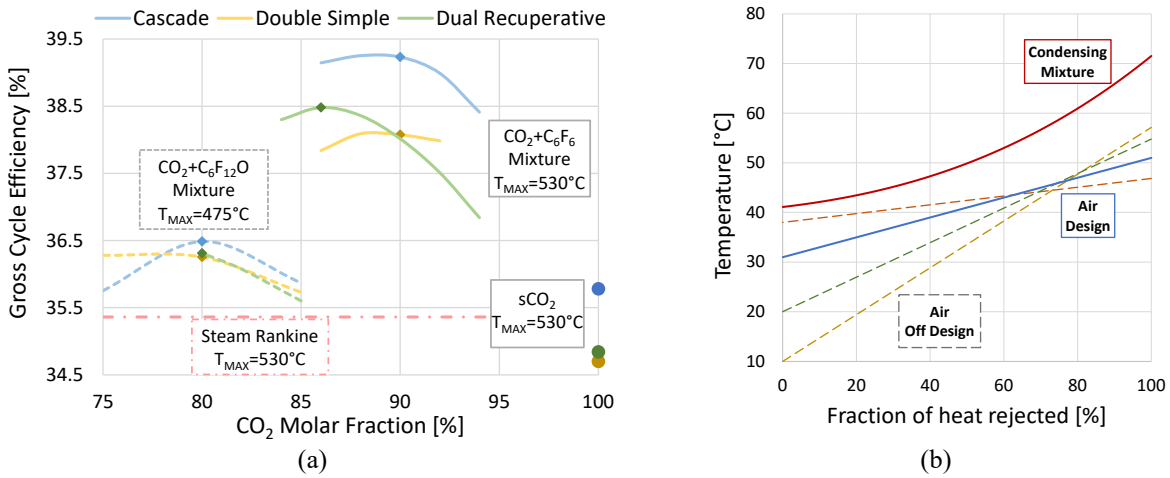

FIGURE 6. Gross cycle efficiency (considering exclusively the compression and expansion work) for various plant layouts, mixtures and mixtures compositions (a), design and off design T-Q diagram of the condenser of the Cascade CO_2+C_6F_6 cycle (b).

Finally, once the design of the innovative power cycles is carried out at an ambient temperature of 31°C and the off-design analysis performed as described, the cycle electromechanical efficiency, the gearbox efficiency and auxiliary consumption of the air cooled condenser can be considered to compute the power block net electric efficiency proposed in Figure 7 (a). The results emphasize both the high performances of the innovative CO_2+C_6F_6 mixture and the competitiveness of the CO_2+ $C_6F_{12}O$ mixture with respect to the steam cycle, considering the lower turbine inlet temperature, reduced by 55°C with respect to the Rankine cycle. Being the cascade cycle the most efficient between the three proposed, Figure 7 (b) presents the Ts diagrams of the two mixtures best efficiency power cycles.

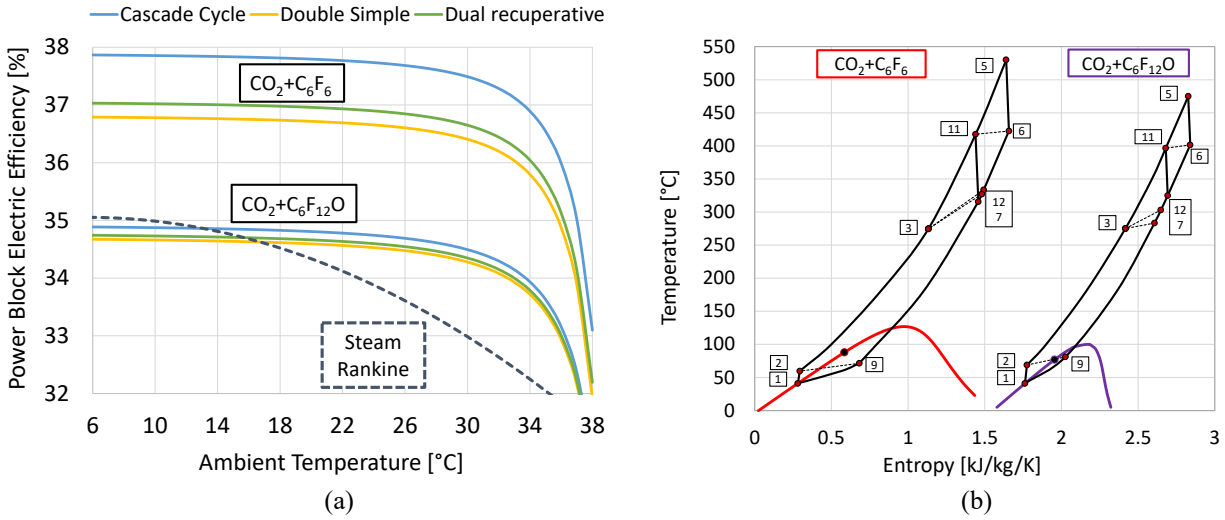

FIGURE 7. Power block net electric efficiency for a wide range of ambient temperature and various plant layouts (a), T-s diagrams of the cascade layout at optimal composition for both the CO_2+C_6F_6 and CO_2+$C_6F_{12}O$ mixture (b) (the s-axis has been arbitrarily scaled to fit the two diagrams in a single figure).

Regarding the CAPEX of the power block, whose modeling is detailed in the previous chapter, the results of the three power block layouts adopting the respective optimal mixture composition are shown in Figure 8. The most significant differences between the two mixtures are the cost of the PHE and PCHE: while the PHE cost is generally lower for the $C_6F_{12}O$ mixture due to the different turbine inlet temperature (the hot end ΔT varies from 15°C to 70°C), the cost of the PCHE, on the other hand, is higher for the $C_6F_{12}O$ mixture due to a lower logarithmic mean temperature difference (ΔT_{ML}) across the PCHEs.

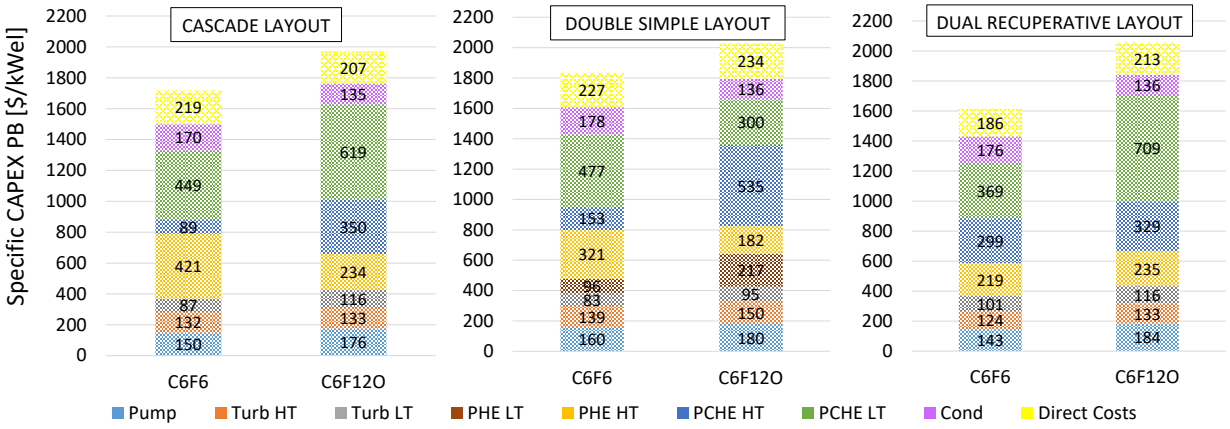

FIGURE 8. Power block CAPEX breakdown for the transcritical cycles analyzed, according to Weiland [11] and Carlson [12].

ENERGY PRODUCTION AND ECONOMIC RESULTS

The resulting yearly energy produced and capacity factors are reported in Table 4, along with a comprehensive review of the capex involved and the LCOE, computed assuming a plant lifetime of 25 years.

TABLE 4. Power plant performances of the various cycle configurations studied: results include energy and economic indicators.

Parameter	Steam Rankine	$CO_2 + C_6F_6$ mixture			$CO_2 + C_6F_{12}O$ mixture		
		Cascade	Double Simple	Dual recuperative	Cascade	Double Simple	Dual recuperative
Electric Energy [GWh]	15.42	17.40	16.84	16.96	16.18	16.08	16.11
Capacity Factor [%]	40.1	44.3	44.1	44.2	44.1	44.8	44.1
Design Power [MW_{el}]	4.11	4.48	4.36	4.38	4.19	4.10	4.17
PB Capex [$/$kW_{el}$]	1400/3000	1718	1834	1616	1970	2029	2055
Solar field [M$]	18.1	18.1	18.1	18.1	18.1	18.1	18.1
Storage cost [M$]	4.5	4.5	4.5	4.5	4.5	4.5	4.5
Indirect+Conting. [M$]	5.0	5.0	5.0	5.0	5.0	5.0	5.0
Specific Capex [$/$kW_{el}$]	8115/9715	7878	8164	7917	8557	8760	8673
LCOE [$/$MWh_{el}$] (Discount rate 8%)	227/266	213	221	214	230	232	233

It can be noticed that a significantly higher annual energy is produced when adopting the innovative cycles, while, on the other hand, more limited economic advantages are shown.

An additional advantage of the innovative proposed cycles, with respect to the Rankine cycle, lies in the cycle heat rejection temperature, since the condensation of mixtures is not an isothermal process. For the two mixtures, an alternative to the air-cooled condenser is proposed: the heat rejection from the cycle can in fact occur into a closed loop of demineralized water, similarly to a water-cooled condenser. In this way it becomes possible to transfer heat to another source at medium temperature for cogeneration purposes, avoiding the use of the air condenser. Assuming demineralized water at the cold end of the condenser entering at 31°C and 4°C of minimum temperature difference across the heat exchanger, the cold source can be heated to feed with thermal power a cogenerative process: in Table 5, the maximum temperature obtainable is listed, along with the seasonal thermal energy recovered.

The power cycle working with the $C_6F_{12}O$ mixture presents a more exploitable rejected heat, carried out at 76°C, 10°C higher than the one exploiting the C_6F_6 mixture. While in winter the heat can be used for cogeneration in a low temperature district heating process, in summer, instead, it can be exploited in a desalination plant, a possibility already

explored in literature [17] using multi effect distillation (MED) as desalination technologies. The avoided parasitic electric load of the air-cooled condenser is, nonetheless, negligible with respect to the yearly electric production.

TABLE 5. Description of the recovered heat from the condenser of the innovative cycles both during the hot and cold periods.

Parameter	$CO_2 + C_6F_6$ mixture			$CO_2 + C_6F_{12}O$ mixture		
	Cascade	Double Simple	Dual recuperative	Cascade	Double Simple	Dual recuperative
Cogenerative source maximum temperature	66°C	66°C	66°C	76°C	76°C	76°C
Summer Thermal load at condenser [GWh]	18.8	19.1	19.0	19.5	20.8	19.6
Winter Thermal load at condenser [GWh]	10	10.2	10.2	10.4	10.4	10.4

CONCLUSION

This work aims at comparing a small-scale steam Rankine cycle with innovative transcritical cycles using CO_2 mixtures as working fluids in CSP plants using LFR. The solar plant, whose design is inspired by a real operating plant, is located in Sicily in a town with a relatively low solar resource. The economic results are preliminary, with the highest uncertainties on the cost functions of the power blocks. In the authors opinion, the reduction in LCOE with respect to the traditional Rankine cycle can be up to 10% (around 213$/MWh) adopting C_6F_6 as dopant, while a similar LCOE is computed if the $C_6F_{12}O$ is used as dopant in the mixture. The yearly energy produced, moreover, increases by 13% for the C_6F_6 mixture and 5% for the $C_6F_{12}O$ mixture. For these reasons, CO_2 mixtures can be very interesting in CSP plants even for small scale applications, easily exceeding the sCO_2 performances, especially when a large temperature difference across the PHE is imposed.

The most significant limit of the analysis proposed is the off-design characterization of the innovative cycles, where a constant cycle minimum temperature is considered along the year. Future developments of this work will model the off-design conditions varying the cycle minimum temperature according to the ambient temperature, since a reasonable gain in terms of yearly energy production can be foreseen, expanding the benefits of adopting CO_2 based mixtures as working fluids as alternative to steam for power production in CSP plants.

ACKNOWLEDGEMENTS

This paper is part of the SCARABEUS project that has received funding from the European Union's Horizon 2020 research and innovation programme under grant agreement No 814985.

REFERENCES

1. M. Mehos *et al.*, "Concentrating Solar Power Gen3 Demonstration Roadmap," *Nrel/Tp-5500-67464*, no. January, pp. 1–140, 2017, doi: 10.2172/1338899.
2. "Scarabeusproject." [Online]. Available: https://www.scarabeusproject.eu/. [Accessed: 01-Oct-2021].
3. M. Binotti, C. M. Invernizzi, P. Iora, and G. Manzolini, "Dinitrogen tetroxide and carbon dioxide mixtures as working fluids in solar tower plants," *Sol. Energy*, vol. 181, no. February, pp. 203–213, 2019, doi: 10.1016/j.solener.2019.01.079.
4. G. Pikra, A. Salim, B. Prawara, A. J. Purwanto, T. Admono, and Z. Eddy, "Development of small scale concentrated solar power plant using organic Rankine cycle for isolated region in Indonesia," *Energy Procedia*, vol. 32, pp. 122–128, 2013, doi: 10.1016/J.EGYPRO.2013.05.016.
5. M. Falchetta *et al.*, "The Partanna Project: A first of a kind plant based on molten salts in LFR collectors," *AIP Conf. Proc.*, vol. 2303, Dec. 2020, 40001, https://aip.scitation.org/doi/abs/10.1063/5.0029269.
6. Y. Li, X. Zhang, S. Tian, S. Xiao, Y. Li, and D. Chen, "Insight into the decomposition mechanism of C6F12O-CO2 gas mixture," *Chem. Eng. J.*, vol. 360, pp. 929–940, Mar. 2019, doi: 10.1016/J.CEJ.2018.10.167.
7. "Home - System Advisor Model (SAM)." [Online]. Available: https://sam.nrel.gov/. [Accessed: 01-Oct-2020].

8. G. Di Marcoberardino, E. Morosini, and G. Manzolini, “Preliminary investigation of the influence of equations of state on the performance of CO2 + C6F6 as innovative working fluid in transcritical cycles,” *Energy*, vol. 238, p. 121815, Jan. 2022, doi: 10.1016/J.ENERGY.2021.121815.
9. K. Jeong, J. Im, S. Lee, and H. Kim, “Vapour + liquid equilibria of the carbon dioxide + pentafluoroethane (HFC-125) system and the carbon dioxide + dodecafluoro-2-methylpentan-3-one (NOVEC^{TM}1230) system,” *J. Chem. Thermodyn.*, vol. 39, no. 4, pp. 531–535, Apr. 2007, doi: 10.1016/J.JCT.2006.09.010.
10. F. Crespi, G. Gavagnin, D. Sánchez, and G. S. Martínez, “Supercritical carbon dioxide cycles for power generation: A review,” *Appl. Energy*, vol. 195, pp. 152–183, Jun. 2017, doi: 10.1016/j.apenergy.2017.02.048.
11. N. T. Weiland, B. W. Lance, and S. R. Pidaparti, “SCO2 power cycle component cost correlations from DOE data spanning multiple scales and applications,” in *Proceedings of the ASME Turbo Expo*, 2019, vol. 9, doi: 10.1115/GT2019-90493.
12. M. D. Carlson, B. M. Middleton, and C. K. Ho, “Techno-Economic Comparison of Solar-Driven sCO2 Brayton Cycles Using Component Cost Models Baselined With Vendor Data and Estimates,” *Proc. ASME 2017 Power Energy Conf.*, pp. 1–7, 2017, doi: 10.1115/ES2017-3590.
13. AACE International recommended Practice, “Cost-Estimate classification system - as applied in Engineering procurement and construction for the process industry,” 2018.
14. “Thermoflow Inc., Thermoflex, (2021). https://www.thermoflow.com/.” [Accessed: 01-Oct-2021].
15. “M.Falchetta, personal communication (09/2021).” .
16. D. Alfani, M. Astolfi, M. Binotti, P. Silva, and E. Macchi, “Off-design performance of CSP plant based on supercritical CO2 cycles,” *AIP Conf. Proc.*, vol. 2303, no. 1, p. 130001, 2020, https://aip.scitation.org/doi/abs/10.1063/5.0029801.
17. P. Sharan, T. Neises, J. D. McTigue, and C. Turchi, “Cogeneration using multi-effect distillation and a solar-powered supercritical carbon dioxide Brayton cycle,” *Desalination*, vol. 459, pp. 20–33, Jun. 2019, doi: 10.1016/j.desal.2019.02.007.